Available online at www.sciencedirect.com

ScienceDirect

Mendeleev Commun., 2018, **28**, 444–446

Mendeleev Communications

Electrochemically synthesized Pt-based catalysts with different carbon supports for proton exchange membrane fuel cell applications

Alexandra B. Kuriganova,*[a] Igor N. Leontyev,[b] Olga A. Maslova[b,c] and Nina V. Smirnova[a]

[a] *Department of Technology, M. I. Platov South-Russian State Polytechnic University, 346428 Novocherkassk, Russian Federation. E-mail: kuriganova_@mail.ru*

[b] *Department of Physics, Southern Federal University, 344006 Rostov-on-Don, Russian Federation*

[c] *Universidade Federal de Minas Gerais, 31270-010 Belo Horizonte, Brazil*

DOI: 10.1016/j.mencom.2018.07.036

The Pt/C catalysts containing various types of carbon support were prepared *via* electrochemical oxidation/dispersion. Their different catalytic activity in CO-stripping and ethanol electrooxidation was revealed.

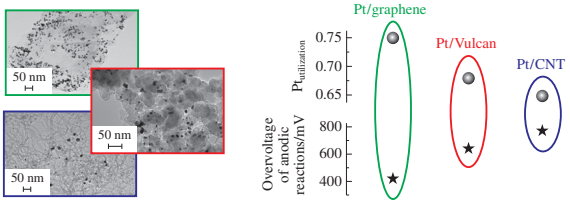

Proton exchange membrane fuel cells are promising for power supply in mobile systems and portable devices. One of the key factors determining their efficiency is the activity of Pt-based catalysts, which are used therein. The Pt-based catalyst is typically composed of platinum nanoparticles deposited onto various carbon supports.[1]

The structure of the carbon support of Pt-based catalysts is one among the essential aspects that influence the catalyst activity in the relevant processes,[2] in addition to the structure of a catalytic layer in membrane electrode assembly and the overall performance of the fuel cell.[3,4] There is a huge amount of the known carbon nanostructures,[5] wherein a carbon black, carbon nanotubes, and graphene demonstrate the best characteristics for using as the supports for platinum group metal based catalysts.[6,7] This work was aimed at the establishment of effects of the carbon support morphology on electrocatalytic performance of Pt/C catalysts, while the platinum particles were prepared *via* the technique used in our previous work[8] to preserve their microstructure characteristics.

We have earlier shown that the Pt/C-catalyst based on carbon soot Vulcan XC-72 possessed a better catalytic activity in both cathodic and anodic processes as compared to the chemically obtained commercial catalyst.[9] Thus, three types of Pt-based catalysts with carbon black, carbon nanotubes and graphene supports were chosen for further investigations. Vulcan XC-72 (Cabot Corp.) was used as carbon black, carbon nanotubes (CNT) were obtained by the pyrolysis of propane–butane mixture on Cu–Ni catalyst, the graphene sample was prepared by an electrochemical dispersion of expanded graphite applying an alternating current. The characteristics of selected carbon supports are summarized in Table 1, while their Raman spectra are shown in Figure 1(*a*). Six bands are observed at 1354, 1581, 1621, 2455, ~2720, and 2945 cm^{-1}, where the first three of them can be assigned to the resonance Raman D-, G- and D′-modes, respectively. The remaining signals [G*-peak, G′(2D)-band, and D+G line] were caused by the double-resonance Raman effect. The D-to-G intensity ratio I_D/I_G related to the defects of density in the sample is also given in Table 1. The parameter I_D/I_G for graphene is much lower than that for carbon black and for nanotubes. It should be noted that the defects are also presented in the graphene crystalline structure and at its edges. The G′-band of synthesized

Table 1 Characteristics of the selected carbon supports.

Carbon support	Geometric parameters	S_{BET}/ $m^2\ g^{-1}$	Raman spectroscopy, I_D/I_G
Vulcan XC-72	Average particle diameter of 30–60 nm	237	1.97
CNT	Outer diameter 0–20 nm, inner diameter 3–8 nm, length > 10 μm	232	2.37
Graphene	Lateral dimensions of 0.5–2 μm	240	0.25

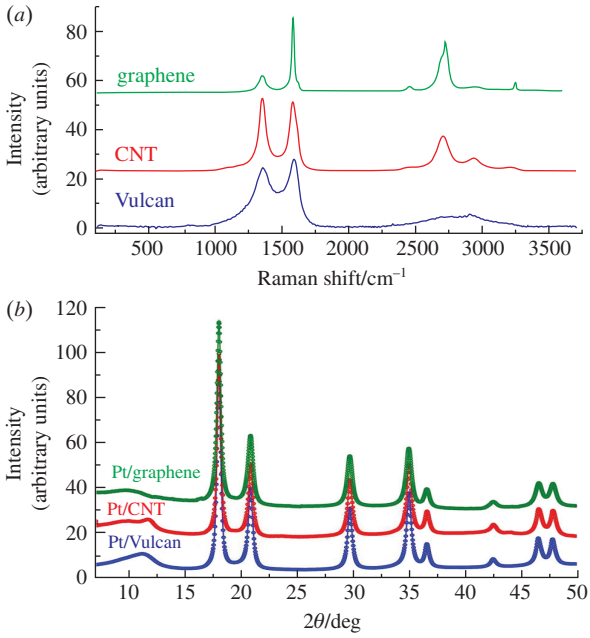

Figure 1 (*a*) Raman spectra of carbon supports and (*b*) XRD patterns of Pt/C catalysts.

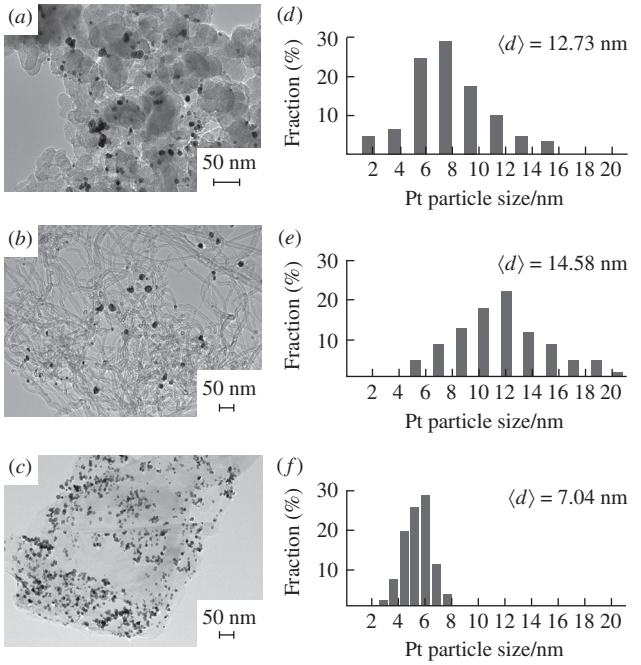

Figure 2 (*a*)–(*c*) TEM images and (*d*)–(*f*) platinum particles size distribution of (*a*),(*d*) Pt/Vulcan, (*b*),(*e*) Pt/CNT and (*c*),(*f*) Pt/graphene catalysts.

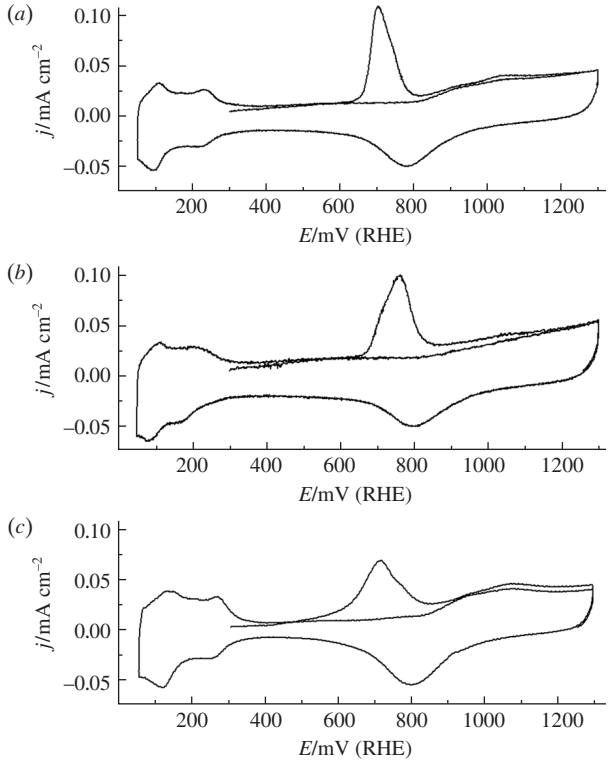

Figure 3 CO stripping on (*a*) Pt/Vulcan, (*b*) Pt/CNT and (*c*) Pt/graphene catalysts; the scan rate was 20 mV s^{-1}; CO was adsorbed at E = 300 mV *vs.* RHE.

graphene consists of 3 peaks at 2650, 2695, and 2728 cm^{-1}. Although its height intensity is much lower than that of G-peak, its shape allows one to conclude that the number of graphene layers in the studied sample varies from 3 to 5.[19–21]

Nanodispersed Pt/C catalysts were prepared *via* electrochemical dispersion of Pt electrodes according to the reported procedures.[8–11] However, one modification was introduced in contrast with ref. 11: the Pt/graphene catalyst was synthesized by sequential electrochemical dispersion of expanded graphite and platinum foil. The platinum loading in the catalysts was 25 ± 0.5%.

X-ray patterns† of all three synthesized Pt/C catalysts are shown in Figure 1(*b*). The reflections corresponding only to the face centered cubic (fcc) structure (space group *Fm*3*m*) were observed for the all samples. The average size of nanoparticles and unit cell parameters determined using Rietveld refrainment[5] are presented in Table 2. It is clearly seen from Table 2 that the unit cell parameter of platinum nanoparticles for all samples is smaller than for bulk platinum due to the surface relaxation in accordance with our previous report.[12]

The TEM images‡ [Figure 2(*a*–*c*)] revealed that the platinum particles were uniformly distributed over the surface of all used carbon supports. However, the presence of agglomerates with sizes greater than 15 nm is more characteristic of the Pt/CNT catalyst [Figure 2(*e*)].

The different morphologies of the catalysts also impacted the CV curves of CO oxidation (Figure 3). The lowest overvoltage of CO oxidation on Pt is typical of the Pt/Graphene catalyst, where both the onset potential (CO_{onset}) and peak potential of CO oxidation (CO_{peak}) belong to a more cathodic range as compared to the Pt/Vulcan catalyst. The important characteristic indicating the efficiency of the platinum surface usage is a $Pt_{utilization}$ parameter,[13] which is the electrochemically active surface area (ECSA) per chemically active surface area (CSA) of the catalyst: $Pt_{utilization}$ = = ECSA/CSA.

The ECSA of Pt-based catalysts was determined *via* CO stripping.[14] The CSA of the catalysts was calculated according to the following equation: $CSA = 6 \times 10^3/pd$, wherein $\langle d \rangle$ is the average platinum particle diameter expressed in nanometer (from TEM measurements) and p is the density of platinum (21.4 g cm^{-2}). The values of ECSA and CSA are listed in Table 2.

The greatest $Pt_{utilization}$ value was demonstrated by the Pt/graphene catalyst (Table 2) due to a more uniform distribution of platinum nanoparticles over the graphene surface [Figure 2(*c*)] in comparison with catalysts based on carbon black Vulcan and carbon nanotubes [Figures 2(*a*) and (*b*), respectively].

The electrocatalytic activity was investigated for the electrochemical oxidation of ethanol. Figure 4 shows the onset CV ranges of Pt-based catalysts in the 0.5 M EtOH + 0.5 M H_2SO_4 solution. An important indicator of activity of Pt-based catalysts is the reduction at overvoltage of the oxidation process. The onset potential of ethanol oxidation $E_{EtOHonset}$ on the Pt/graphene catalyst

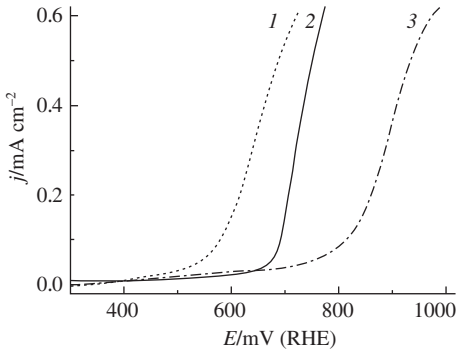

Figure 4 Onset in CV curves of Pt-based catalysts: (*1*) Pt/graphene, (*2*) Pt/Vulcan, (*3*) Pt/CNT in the 0.5 M EtOH + 0.5 M H_2SO_4 solution acquired at a scan rate of 5 mV s^{-1}.

† X-ray measurements were carried out at the Swiss-Norwegian beam lines of the European Synchrotron radiation facility at the radiation wavelength λ = 0.694724 Å using a 2-D Pilatus2M (Dectris) detector.

‡ The particle size distribution was obtained *via* transmission electron microscopy (TEM) on a Hitachi HT-7700 TEM (High-Technologies Europe GmbH) system at the field emission of 100 kV.

The Raman measurements were performed on a micro-Raman system inVia Reflex Renishaw in a back-scattering configuration using argon laser at the wavelength of 488 nm.

Table 2 Microstructural and electrochemical properties of the prepared catalysts.

Catalyst	D_{111}/nm	D_{100}/nm	a/Å	$\langle d \rangle$/nm	CSA/m^2 g^{-1}	ECSA/m^2 g^{-1}	ECSA/CSA	E_{COonset}/mV	E_{COpeak}/mV	$E_{\mathrm{EtOHonset}}$/mV
Pt/Vulcan	10.6	7.6	3.9168	12.73	22.0	15.0	0.68	600	703	637
Pt/CNT	7.6	6.0	3.9153	14.58	19.2	12.6	0.65	634	761	772
Pt/graphene	7.6	5.2	3.9178	7.04	39.8	30.1	0.75	481	712	417

is shifted towards the cathodic range by 135 mV as compared to the Pt/Vulcan catalyst (Table 2), which is the pronounced decrease in overvoltage. On the Pt/CNT catalyst, the ethanol oxidation occurred at a significant overvoltage (see Figure 4 and Table 2), which could be caused by the different ECSA/CSA values for all three catalysts since the platinum surface might partially become electrochemically inactive due to agglomeration and unavailability for reagents.[15–18]

Therefore, the microstructural and electrochemical characteristics of Pt-based catalysts obtained *via* electrochemical oxidation/dispersion are mainly determined by the type of selected carbon support. The greatest value of the $\mathrm{Pt}_{\mathrm{utilization}}$ parameter was demonstrated by the graphene-based catalyst, which explains its excellent electrochemical characteristics in the electrooxidation of CO and ethanol.

Electrochemical tests were performed using equipment of the Shared Research Center ‘Nanotechnologies’ of the M. I. Platov South-Russian State Polytechnic University.

This work was supported by the Ministry of Education and Science of the Russian Federation (state contract no. 14.587.21.0029, identification no. RFMEFI58716X0029).

References

1 P. Trogadas, T. F. Fuller and P. Strasser, *Carbon*, 2014, **75**, 5.
2 A. N. Kalenchuk, N. A. Davshan, V. I. Bogdan, S. F. Dunaev and L. M. Kustov, *Russ. Chem. Bull., Int. Ed.*, 2018, **67**, 28 (*Izv. Akad. Nauk, Ser. Khim.*, 2018, 28).
3 E. V. Gerasimova, E. Yu. Safronova, A. A. Volodin, A. E. Ukshe, Yu. A. Dobrovolsky and A. B. Yaroslavtsev, *Catal. Today*, 2012, **193**, 81.
4 R. S. Batalov, V. V. Kuznetsov, B. I. Podlovchenko and V. A. Zaytsev, *Mendeleev Commun.*, 2017, **27**, 583.
5 E. Antolini, *Appl. Catal., B.*, 2009, **88**, 1.
6 S. D. Kushch, N. S. Kuyunko, A. A. Arbuzov and G. V. Bondarenko, *Kinet. Catal.*, 2015, **56**, 818 (*Kinet. Katal.*, 2015, **56**, 808).
7 A. A. Arbuzov, S. A. Mozhzhukhin, A. A. Volodin, P. V. Fursikov and B. P. Tarasov, *Russ. Chem. Bull., Int. Ed.*, 2016, **65**, 1893 (*Izv. Akad. Nauk, Ser. Khim.*, 2016, 1893).
8 A. B. Kuriganova and N. V. Smirnova, *Mendeleev Commun.*, 2014, **24**, 351.
9 I. Leontyev, A. Kuriganova, Y. Kudryavtsev, B. Dkhil and N. Smirnova, *Appl. Catal., A*, 2012, **431**–**432**, 120.
10 A. B. Kuriganova, I. N. Leontyev, A. S. Alexandrin, O. A. Maslova, A. I. Rakhmatullin and N. V. Smirnova, *Mendeleev Commun.*, 2017, **27**, 67.
11 A. B. Kuriganova, I. N. Leontyev, M. V. Avramenko, Yu. Popov, O. A. Maslova, O. Yu. Koval and N. V. Smirnova, *ChemistrySelect*, 2017, **2**, 6979.
12 I. N. Leontyev, A. B. Kuriganova, N. G. Leontyev, L. Hennet, A. Rakhmatullin, N. V. Smirnova and V. Dmitriev, *RSC Adv.*, 2014, **4**, 35959.
13 J. Perez, V. A. Paganin and E. Antolini, *J. Electroanal. Chem.*, 2011, **654**, 108.
14 M. J. Watt-Smith, J. M. Friedrich, S. P. Rigby, T. R. Ralph and F. C. Walsh, *J. Phys. D: Appl. Phys.*, 2008, **41**, 174004.
15 W. Li, W. Zhou, H. Li, Z. Zhou, B. Zhou, G. Sun and Q. Xin, *Electrochim. Acta*, 2004, **49**, 1045.
16 F. Colmati, E. Antolini and E. R. Gonzalez, *Electrochim. Acta*, 2005, **50**, 5496.
17 S. L. Knupp, W. Li, O. Paschos, T. M. Murray, J. Snyder and P. Haldar, *Carbon*, 2008, **46**, 1276.
18 S. Eris, Z. Daşdelen and F. Sen, *J. Colloid Interface Sci.*, 2018, **513**, 767.

Received: 4th October 2017; Com. 17/5367